Global Reaction Kinetics and Enthalpy in Slow Pyrolysis of Vegetal Materials

TANASE DOBRE[1], OANA CRISTINA PARVULESCU[1*], INMACULADA RODRIGUEZ RAMOS[2], LAURENTIU CEATRA[1], MARTA STROESCU[1], ANICUTA STOICA[1], RADU MIREA[1]

[1]Politehnica University of Bucharest, Chemical Engineering Department, 1-3 Polizu, 011061, Bucharest, Romania
[2]Institute of Catalysis and Petrochemistry, Group for Molecular Design of Heterogeneous Catalysts, Madrid, Spain

Fixed bed pyrolysis of corn grains impregnated or not with a nickel nitrate solution was performed under carbon dioxide atmosphere, obtaining permanent gases, a pyrolytic oil and a solid residue (char). The distribution of pyrolysis products was dependent on variations in heat flux, carbon dioxide superficial velocity, grain size and impregnation degree. Correlations between these factors and process dependent variables, i.e. char mass, oil mass, operation time, material bed centre temperature and column wall temperature, were established using a 2^3 factorial plan. A one-stage global reaction kinetic model was selected to describe the process dynamics. An unsteady state model based on heat and mass transfer from solid particles to gaseous phase was adopted to estimate the global reaction enthalpy. The results obtained may provide useful data for the design, scaling-up, optimization and operation of fixed bed pyrolysis reactors.

Keywords: pyrolysis, biomass, factorial experiment, kinetic model, reaction enthalpy

Vegetal materials pyrolysis, consisting of solid thermal degradation without oxygen, is usually performed in presence of a carrier gas which can be inert (nitrogen, argon) or oxidant (carbon dioxide, steam). The pyrolysis products are lumped into three groups: permanent gases, a pyrolytic liquid (bio-oil/tar) and a solid residue (char), or simply into volatiles and char. These fractions result from both primary reactions of solid material devolatilization and secondary reactions of primary products degradation, i.e. char aromatization and cracking of condensable volatile organic compounds into low molecular weight gases [1-6]. The pyrolytic gas and bio-oil can be employed as combustibles or raw materials sources, whereas the char is useful as a renewable fuel, activated carbon or catalyst support.

The pyrolysis rate as well as the yields, composition and properties of the pyrolysis products depend on numerous factors, e.g. heating rate, process temperature, operation time, type and flow rate of carrier gas, raw material properties (chemical composition, size, shape, density, pretreatment) etc. An increase in volatiles production and a decrease in char amount with heating rate increasing were reported [6-8].

Referring to the process temperature influence, it is obvious that an increase in operation temperature produces a decrease in char yield as well as an enlargement of volatiles yield. At temperatures less than 500^0C, incondensable gases and oil production increases with temperature increasing, whereas at temperatures higher than 500^0C, gas yield increases and oil yield decreases with temperature increasing, as effect of an enhancement of oil vapour cracking [4,6-17].

The size of biomass particles has a significant effect on products yield. Accordingly, an increase in grain size determines temperature gradients in the particle, so the temperature at the centre is lower than that at the surface, resulting an increase in solid amount and a decrease in oil production [4,6,18]. At temperatures higher than 500^0C, smaller particles favour the oil vapour cracking reactions with an increase in incondensable gases production, because the volatiles residence time in the reactor is longer when smaller particles are used [6]. Generally, particles sizes less than 1.3 mm do not affect the pyrolysis products yield [9,18].

Biomass chemical pretreatment has an important effect on the process dynamics. Vegetal structure pretreatment with various activating agents, i.e. zinc chloride, sodium carbonate, potassium carbonate, leads to a high oil yield, due to an enhancement of intramolecular dehydration reactions in the impregnated material [10,11,14]. An important production of hydrogen-rich pyrolytic gas can be obtained starting by a vegetal material pretreated with a nickel nitrate solution [1,5]. Some reactions occurring during the pyrolysis of nickel nitrate impregnated biomass are [5,19,20]: (I) breaking of vegetal structure polymer chains producing char, hydrocarbons, carbon dioxide, water and carbon; (II) reforming of generated hydrocarbons leading to syngas; (III) cracking of support and hydrocarbons; (IV) oxidation of carbon (C^0) to carbon monoxide (C^{+2}); (V) decomposition of nickel nitrate impregnated into porous structure in nickel oxide, nitrogen dioxide and oxygen; (VI) reduction of nickel oxide (Ni^{+2}) to metallic nickel (Ni^0); (VII) consumption of nitrogen dioxide by reactions with carbon or other gases. During pyrolysis, metallic nickel (Ni^0) nanocrystallites are formed into porous vegetal structure, as demonstrated by X-ray diffraction (XRD), X-ray photoelectron spectroscopy (XPS), transmission electron microscopy (TEM) and temperature-programmed pyrolysis experiments [5]. These Ni^0 nanocrystallites act as a catalyst and activate some of the pyrolytic reactions, e.g. reforming, cracking and nitrogen dioxide consumption.

Simple or more complex models have been proposed to describe the process dynamics. Simple kinetic models can be classified into three categories: one-stage (one-reaction) global, multi-stage (multi-reaction) global and semi-global models [2,3,21,22]. One-stage global kinetic models consider pyrolysis as a single first order reaction:

$$Vegetal\ material \xrightarrow{k} volatiles + char$$

* email: oana.parvulescu@yahoo.com; Tel.: (+40) 021 402 38 10

Set	Exp	q (W/m^2)	w (m/h)	d (cm)	c (g/L)	Set	Exp	q (W/m^2)	w (m/h)	d (cm)	c (g/L)
1	1	2600	1	0.8	0	2	9	2600	1	0.8	300
	2	2600	2	0.8			10	2600	2	0.8	
	3	3470	1	0.8			11	3470	1	0.8	
	4	3470	2	0.8			12	3470	2	0.8	
	5	2600	1	0.4			13	2600	1	0.4	
	6	2600	2	0.4			14	2600	2	0.4	
	7	3470	1	0.4			15	3470	1	0.4	
	8	3470	2	0.4			16	3470	2	0.4	

Table 1
PROCESS FACTORS LEVELS

The reaction rate constant, k, is written in terms of pre-exponential factor and activation energy according to Arrhenius equation. Multi-stage global kinetic models contain parallel and successive primary reactions of degradation of the main biomass constituents. Semi-global kinetic models include both primary decomposition reactions, producing volatiles and char, and degradation reactions of primary products into secondary pyrolysis products. More complex models are based on kinetic equations coupled with mass, heat and momentum transport equations [2,3,12,22-25].

This paper focuses on the qualitative and quantitative characterization of fixed bed pyrolysis of corn grains impregnated or not with a nickel nitrate solution, in the presence of a carbon dioxide stream.

Experimental part

Materials

Untreated and Ni (II) impregnated corn grains were employed as vegetal material. The metallic salt used for the grains impregnation was [$Ni(NO_3)_2 . 6H_2O$]. Whole and crushed corn grains were stirred with a nickel nitrate aqueous solution at a concentration of 300 g/L. Batch impregnation was performed for 72 h at a solid-liquid ratio of 1:5. The corn grains were then filtered and dried in an oven at 105 ^{0}C for 72 h.

Equipment and procedure

The laboratory set-up used for pyrolysis process study was described in our previous studies [19,20,26]. A 400 g sample of vegetal material was introduced in a 5 cm diameter and 50 cm height quartz column. The column wall was heated by an electric resistance with a preset heat flow. The carbon dioxide from a cylinder, whose flow was measured by a flow-meter and controlled by a pressure reducer, was fed into the column by a pipe, up-flowed through the material fixed bed and was evacuated with the volatiles obtained during the pyrolysis. The mixture of gases and vapours was cooled in a condenser, producing pyrolytic oil and incondensable gases. Vegetal material mass, oil mass, bed centre temperature and column wall temperature were recorded and collected by a data acquisition system.

Experimental variables

Experimental investigation was performed at two values (levels) of process independent variables (factors), i.e. heat flux, q, carbon dioxide superficial velocity, w, mean volume equivalent diameter of corn grain, d, and nickel nitrate solution concentration, c. Two sets of 8 experiences were performed according to a 2^3 factorial plan (table 1). Vegetal material mass, m, oil mass, m_{oil}, bed centre temperature, t_c, and column wall temperature, t_w, were continuously recorded as a function of heating time, τ. Each experience was replicated three times to determine its reproducibility, which was found to be good.

Results and discussions

Experimental data

Time variation curves of vegetal material mass, m/m_0, given in figure 1, and oil mass, m_{oil}/m_0, shown in figure 2, have the same shape of bent step. As expected, a decrease in char yield and an enlargement of oil production occur at

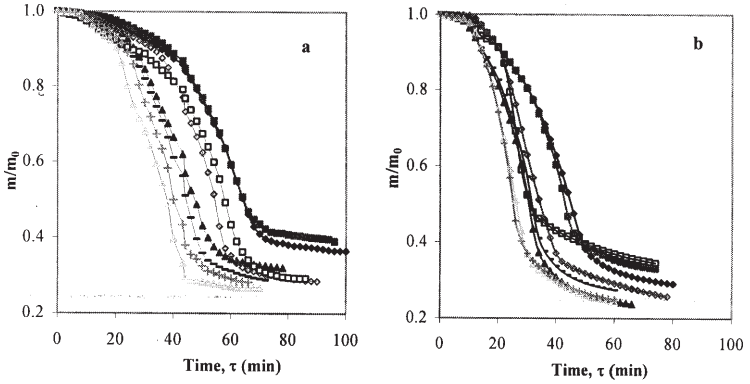

Fig. 1. Time evolution of vegetal material mass during pyrolysis:
a-experimental set 1
♦ exp 1,■ exp 2, ▲ exp 3, – exp 4,
◊ exp 5, □ exp 6, △exp 7, + exp 8); b-experimental set 2 (♦ exp 9, ■ exp 10, ▲ exp 11, – exp 12, ◊exp 13, □ exp 14, △exp 15, + exp 16)

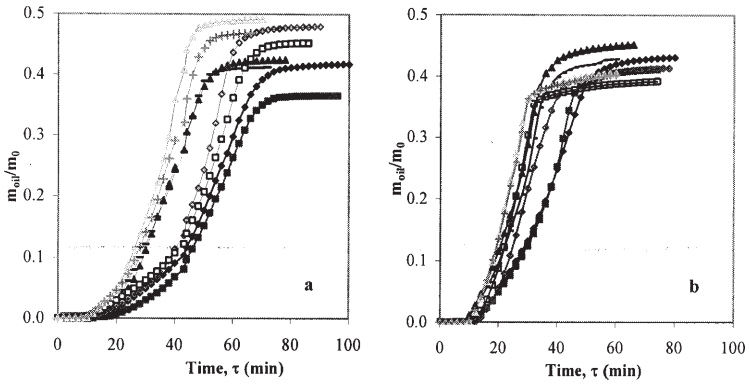

Fig. 2. Time evolution of oil mass during pyrolysis:
a-experimental set 1
♦ exp 1,■ exp 2, ▲ exp 3, – exp 4,
◊ exp 5, □ exp 6, △exp 7, + exp 8); b-experimental set 2 (♦ exp 9, ■ exp 10, ▲ exp 11, – exp 12, ◊exp 13, □ exp 14, △exp 15, + exp 16)

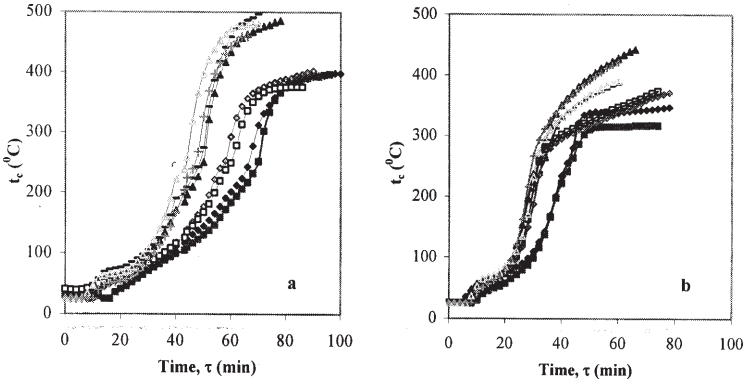

Fig. 3. Time evolution of material bed centre temperature during pyrolysis: a-experimental set 1 ♦ exp 1,■ exp 2, ▲ exp 3, – exp 4, ◊ exp 5, □ exp 6, △exp 7, + exp 8); b-experimental set 2 (♦ exp 9, ■ exp 10, ▲ exp 11, – exp 12, ◊exp 13, □ exp 14, △exp 15, + exp 16)

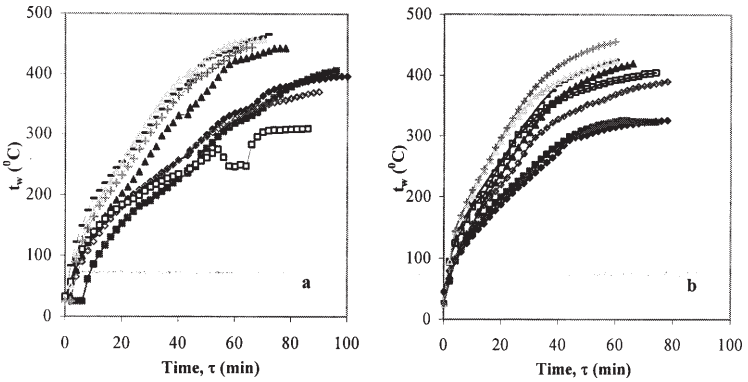

Fig. 4. Time evolution of material column wall temperature during pyrolysis: a-experimental set 1 ♦ exp 1,■ exp 2, ▲ exp 3, – exp 4, ◊ exp 5, □ exp 6, △exp 7, + exp 8); b-experimental set 2 (♦ exp 9, ■ exp 10, ▲ exp 11, – exp 12, ◊exp 13, □ exp 14, △exp 15, + exp 16)

a high value of heat flux. Grain size is an important variable that affects the untreated material pyrolysis (experimental set 1). Accordingly, an increase in grain size determines an increase in solid amount (fig. 1a) and a decrease in oil production (fig. 2a). Referring to the impregnation influence on process performances, it is observed that:

-impregnated grains pyrolysis generally leads to a lower char amount;

-the oil amount produced by impregnated structure pyrolysis is higher than in the case of untreated material, then it attains a constant plateau and characteristic oil mass values of untreated solid become larger; this occurs because the dehydration reactions in the impregnated structure are enhanced at temperatures lower than 350^{0}C, whereas at temperatures higher than 350^{0}C the nickel catalyst activates the decomposition reactions of oil vapour obtained during the pyrolysis, promoting the incondensable gases yield.

Figure 3, which shows temperature dynamics of material bed centre, t_c, indicates that centre temperature increases with heat flux increasing. In case of untreated structure (fig. 3a), it increases with grain size decreasing and is almost invariant with gas velocity. The impregnation produces a sharp increase of bed centre temperature until 250-350^{0}C, followed by a constant plateau, which is probably due to the endothermic reactions of catalytic reforming and cracking. Time variation curves of column wall temperature t_w, illustrated in figure 4, prove that wall temperature increases with heat flux increasing. In case of impregnated structure (fig. 4b), it increases with grain size decreasing.

Characteristic curves of mass and temperature dynamics highlight that the pyrolysis process is more rapid at high level of heat flux and in case of impregnated biomass.

Process modelling

By means of adequate mathematical models, the experimental data plotted in figures 1-4 were employed for quantitative pyrolysis characterization. Three models, i.e. a statistical one, a one-stage global reaction kinetic model and a kinetic model coupled with heat and mass transfer equations, were selected for reported data capitalization.

Statistical model

A statistical model based on a 2^3 factorial plan was used to establish the dependences between the final process responses, namely char mass, $y_1 = m_f / m_o$, oil mass, $y_2 = m_{oilf} / m_o$, operation time, $y_3 = \tau_f / m_o$,bed centre temperature, $y_4 = t_{cf} / m_\rho$,and column wall temperature $y_5 = t_{wf} / m_o$, and dimensionless process factors expressed by equations system:

$$x_1 = \frac{q-3035}{435},\ x_2 = \frac{w-1.5}{0.5},\ x_3 = \frac{d-0.6}{0.2} \qquad (1)$$

Table 2, which contains characteristic data of experimentation matrix, was used to obtain dependences $y_1 = y_i(x_1, x_2, x_3, x_1x_2, x_1x_3, x_2x_3, x_1x_2x_3,)$, i=1...5, given by equations systems:

Experimental set 1 (untreated material)

$$y_1 = 0.312 - 0.022x_1 + 0.002x_2 + 0.030x_3 - 0.006x_1x_2 - 0.015x_1x_3 - 0.004x_2x_3 - 0.008x_1x_2x_3$$

$$y_2 = 0.439 + 0.014x_1 - 0.014x_2 - 0.034x_3 + 0.006x_1x_2 + 0.003x_1x_3 - 0.002x_2x_3 + 0.004x_1x_2x_3$$

$$y_3 = 0.228 - 0.030x_1 - 0.006x_2 - 0.002x_3 - 0.001x_1x_2 - 0.001x_1x_2x_3 \qquad (2)$$

$$y_4 = 1.214 + 0.122x_1 - 0.013x_2 - 0.050x_3 + 0.008x_1x_2 + 0.003x_1x_3 + 0.022x_2x_3 + 0.003x_1x_2x_3$$

$$y_5 = 1.141 + 0.116x_1 - 0.017x_2 - 0.023x_3 + 0.022x_1x_2 - 0.046x_1x_3 + 0.038x_2x_3 - 0.013x_1x_2x_3$$

Experimental set 2 (impregnated material)

$$y_1 = 0.278 - 0.027x_1 + 0.021x_2 + 0.005x_3 - 0.010x_1x_2 - 0.002x_2x_3 + 0.009x_1x_2x_3$$

$$y_2 = 0.418 + 0.005x_1 - 0.008x_2 + 0.014x_3 + 0.002x_1x_2 + 0.004x_1x_3 - 0.002x_2x_3 - 0.003x_1x_2x_3$$

$$y_3 = 0.198 - 0.022x_1 - 0.004x_2 + 0.007x_3 + 0.002x_1x_2 + 0.001x_1x_3 - 0.005x_2x_3 - 0.002x_1x_2x_3 \quad (3)$$

$$y_4 = 1.079 + 0.083x_1 - 0.020x_2 + 0.018x_3 - 0.001x_1x_2 + 0.039x_1x_3 - 0.045x_2x_3 - 0.018x_1x_2x_3$$

$$y_5 = 1.121 + 0.100x_1 + 0.018x_2 - 0.019x_3 + 0.007x_1x_2 + 0.043x_1x_3 - 0.014x_2x_3 - 0.003x_1x_2x_3$$

Set	Exp.	q (W/m^2)	w (m/h)	d (cm)	c (g/L)	x_1	x_2	x_3	y_1	y_2	y_3 (min/g)	y_4 (^{0}C/g)	y_5 (^{0}C/g)
1	1	2600	1	0.8	0	-1	-1	1	0.365	0.418	0.261	1.040	1.037
	2	2600	2	0.8		-1	1	1	0.391	0.366	0.251	1.036	1.060
	3	3470	1	0.8		1	-1	1	0.321	0.425	0.204	1.268	1.158
	4	3470	2	0.8		1	1	1	0.288	0.413	0.188	1.309	1.218
	5	2600	1	0.4		-1	-1	-1	0.285	0.480	0.265	1.185	1.091
	6	2600	2	0.4		-1	1	-1	0.293	0.453	0.253	1.106	0.911
	7	3470	1	0.4		1	-1	-1	0.267	0.491	0.206	1.412	1.345
	8	3470	2	0.4		1	1	-1	0.283	0.469	0.194	1.353	1.307
2	9	2600	1	0.8	300	-1	-1	1	0.290	0.432	0.235	1.021	0.959
	10	2600	2	0.8		-1	1	1	0.331	0.412	0.217	0.931	0.959
	11	3470	1	0.8		1	-1	1	0.237	0.452	0.194	1.303	1.236
	12	3470	2	0.8		1	1	1	0.275	0.429	0.176	1.134	1.253
	13	2600	1	0.4		-1	-1	-1	0.258	0.414	0.217	1.009	1.062
	14	2600	2	0.4		-1	1	-1	0.343	0.393	0.212	1.025	1.105
	15	3470	1	0.4		1	-1	-1	0.243	0.406	0.163	1.063	1.155
	16	3470	2	0.4		1	1	-1	0.250	0.403	0.174	1.147	1.238

Table 2
EXPERIMENTATION MATRIX

Kinetic model

The second model used for experimental data capitalization is a one-stage global reaction kinetic model. It is recommended to describe the conversion process of raw material to char and volatiles [2,3,8,27-30]. For dynamic data obtained at a constant heating rate, $\beta = dt_m / d\tau$ where t_m is logarithmic mean temperature between bed centre temperature, t_c, and column wall temperature, t_w, the decomposition rate can be expressed by equation [30]:

$$\frac{d\alpha}{d\tau} = (1-\alpha)\frac{A}{\beta}exp\left(-\frac{E}{RT_m}\right) \quad (4)$$

Characteristic values of pre-exponential factor, A/β, and activation energy, E, which were regressed by experimental data, are given in table 3. Table 3 contains also the mean values of heating rate, β, as well as the ranges of logarithmic mean temperature, t_m, and volatiles conversion, α, wherein the mean values of β were estimated.

In case of untreated material two decomposition stages were identified. The first stage, in the temperature range 102-280 ^{0}C, can be attributed to the starch degradation in floury endosperm, whereas the second stage, in the range 202-344 ^{0}C, can be an effect of the starch degradation in horny endosperm [20,26]. In compliance with data reported in the related literature, only a decomposition stage was observed for impregnated material [31]. Data listed in table 3 highlight an increase of activation energy with heat flux and grain size decreasing whereas the pre-exponential factor increases with grain size decreasing.

Exp.	$\beta=dt_m/d\tau$ (^{0}C/s)	t_m (^{0}C)	α	A/β (1/s)	E (kJ/mol)
	1st decomposition stage				
1	0.079	197-244	0.29-0.52	1.22	30.96
2	0.060	121-194	0.10-0.38	31.32	41.70
3	0.110	183-275	0.28-0.70	0.22	22.71
4	0.129	216-280	0.36-0.61	0.72	28.56
5	0.071	146-199	0.13-0.37	3356.50	69.29
6	0.054	132-184	0.15-0.32	169.40	48.81
7	0.076	141-171	0.13-0.34	23568.25	62.18
8	0.076	102-175	0.05-0.34	184.15	45.33
	2nd decomposition stage				
1	0.080	255-292	0.57-0.85	182527.37	82.97
2	0.080	203-271	0.43-0.87	784.20	55.65
3	0.182	289-351	0.75-0.88	0.43	24.55
4	0.134	290-344	0.69-0.90	23.85	43.47
5	0.108	246-283	0.60-0.88	1568539.42	90.03
6	0.080	202-279	0.41-0.89	13720.63	67.66
7	0.156	250-326	0.62-0.96	18520.90	71.55
8	0.159	218-298	0.51-0.86	83.75	46.02
Exp.					
9	0.147	163-316	0.32-0.87	0.70	26.62
10	0.135	160-295	0.29-0.86	4.45	33.64
11	0.175	133-310	0.20-0.82	0.47	23.76
12	0.183	166-305	0.29-0.81	0.96	27.26
13	0.210	159-311	0.24-0.84	0.02	31.70
14	0.222	158-293	0.19-0.79	0.20	37.81
15	0.188	167-290	0.33-0.83	0.53	27.19
16	0.163	118-281	0.08-0.80	1.60	29.71

Table 3
EFFECT OF PROCESS FACTORS ON KINETIC PARAMETERS

Set	Exp.	q (W/m^2)	w (m/h)	d (cm)	c (g/L)	x_1	x_2	x_3	a x 10^{-4} (J/kg)	b (J/kg grd)
1	1	2600	1	0.8	0	-1	-1	1	39.7	192.1
	2	2600	2	0.8		-1	1	1	35.9	173.6
	3	3470	1	0.8		1	-1	1	35.3	170.7
	4	3470	2	0.8		1	1	1	34.8	168.2
	5	2600	1	0.4		-1	-1	-1	34.4	166.5
	6	2600	2	0.4		-1	1	-1	43.8	211.8
	7	3470	1	0.4		1	-1	-1	41.4	200.2
	8	3470	2	0.4		1	1	-1	31.8	153.8
2	9	2600	1	0.8	300	-1	-1	1	36.2	175.6
	10	2600	2	0.8		-1	1	1	33.6	162.7
	11	3470	1	0.8		1	-1	1	27.1	130.8
	12	3470	2	0.8		1	1	1	29.4	141.7
	13	2600	1	0.4		-1	-1	-1	18.9	91.6
	14	2600	2	0.4		-1	1	-1	12	58.0
	15	3470	1	0.4		1	-1	-1	18.2	88.2
	16	3470	2	0.4		1	1	-1	13.7	66.1

Table 4
EXPERIMENTATION MATRIX AND VALUES OF a, b PARAMETERS

Kinetic model coupled with heat and mass transfer equations

The third model relating to data capitalization is a one-stage global reaction kinetic model coupled with heat and mass transfer equations in fixed bed. Model assumptions were adopted as follows: i) the heat input at the column wall is preponderant taken by solid material; ii) the global reaction enthalpy is generated by pyrolysis reactions occurring in solid phase; iii) the gas flows through the fixed bed with axial dispersion and it is heated by heat transfer from solid phase; iv) the gas flow rate increases into the fixed bed due to the pyrolysis reactions.

Depending on assumptions considered, the model equations consist of:

- heat balance in solid phase:

$$\frac{dt_s}{d\tau} = \frac{4}{D}\frac{q}{\rho_s c_{p,s}(1-\varepsilon)} - \frac{6}{d}\frac{k_h(t_s - t_g)}{\rho_s c_{p,s}} - \frac{v_r \Delta H_r}{c_{p,s}} \quad (5)$$

- heat balance in gaseous phase:

$$\varepsilon\frac{\partial t_g}{\partial \tau} + w\frac{\partial t_g}{\partial z} = D_a\frac{\partial^2 t_g}{\partial z^2} + \frac{6(1-\varepsilon)}{d}\frac{k_h(t_s - t_g)}{\rho_g c_{p,g}} \quad (6)$$

- global reaction rate:

$$v_r = \frac{d\alpha}{d\tau} = (1-\alpha)\frac{A}{\beta}exp\left(-\frac{E}{RT_m}\right) \quad (7)$$

- global reaction enthalpy as a linear dependence on solid phase temperature:

$$\Delta H_r = a - bt_s \quad (8)$$

- total mass balance in solid and gaseous phases:

$$\frac{dw}{dz} = \frac{22.4(t_g + 273)}{273M_g}(1-\varepsilon)\rho_s v_r \quad (9)$$

The following model restrictions were selected:

- initial condition:

$$\tau = 0, 0 \le z \le H, t_g = t_s = t_0, \alpha = 0 \quad (10)$$

- boundary conditions:

$$\tau > 0, z = 0, D_a dt_g / dz = w_0(t_g - t_0) \quad (11)$$

$$\tau > 0, z = H, dt_g / dz = 0 \quad (12)$$

Minimizing the objective function described by relationship (13), the values of a and b parameters were identified for each one of pyrolysis experiments (table 4). Larger values of a and b parameters are emphasized in case of untreated material.

$$F(a,b) = \sum_{i=1}^{n}\left((t_{ci}t_{wi})^{1/2} - \left(t_{si}(a - bt_{si})t_{gi}(a - bt_{si})\right)^{1/2}\right)^2 \quad (13)$$

Conclusions

An experimental set-up was designed and scaled-up in order to study the fixed bed pyrolysis of corn grains. Slow pyrolysis of corn grains impregnated or not with a nickel nitrate solution was conducted. Carbon dioxide was employed as a carrier agent and a reactant in the pyrolysis process. A char, a pyrolytic oil and a gaseous fraction were produced.

A process analysis by 2^3 factorial programming was performed with the factors being heat flux, carbon dioxide superficial velocity and grain size. Correlations between these factors and process dependent variables, namely char mass, oil mass, operation time, char bed temperature and column wall temperature were established. A one-stage global reaction kinetic model, whose parameters were regressed from experimental data, was selected to simulate the process dynamics. An unsteady state model based on heat and mass transfer from solid particles to gaseous phase was adopted to estimate the global reaction enthalpy. The models predicted well the real conditions and they could facilitate the design, scaling-up, optimization and operation of fixed bed pyrolysis reactors.

Acknowledgements: This work was supported by POSDRU ID project nr. 5159/ 2008.

Nomenclature

A/β - pre-exponential factor, 1/s
c - nickel nitrate solution concentration, g/L
c_p - specific heat capacity, J/kg K
d - equivalent spherical diameter of corn grain, m
D - fixed bed diameter, m
D_a - axial dispersion coefficient, m^2/s
E - activation energy, J/mol
H - fixed bed height, m
k_h - partial heat transfer coefficient, m/s
m - vegetal material mass, g
m_{oil} - pyrolytic oil mass, g
M - molecular mass, kg/mol
q - heat flux, W/m^2
R - gas universal constant, R=8.314 J/mol K
t - temperature, ^{0}C
T - absolute temperature, K
v_r - global reaction rate, 1/s
w - carbon dioxide superficial velocity, m/s

x_i - process dimensionless factor, i=1…3
y_j - process final response, j=1…5
z - fixed bed axial coordinate, m

Greek letters

α - volatiles conversion, $\alpha = \frac{m_0 - m}{m_0 - m_f}$

β - heating rate, $\beta = \frac{dt_m}{d\tau}$, ^{0}C/s

ΔH_r - global reaction enthalpy, J/kg

ε - fixed bed void fraction

δ - density, kg/m^3

τ - time, s

Subscripts

c - centre
f - final
g - gas
m - logarithmic mean
s - solid
w - wall
0 - initial

References

1. BRU, K., BLIN, J., JULBE, A., VOLLE, G., J. Anal. Appl. Pyrolysis, **78**, 2007, p. 291
2. Di BLASI, C., J. Anal. Appl. Pyrolysis, **47**, 1998, p. 43
3. Di BLASI, C., Prog. Energy Combust. Sci., **34**, 2008, p. 47
4. PARIHAR, M.F., KAMIL, M., GOYAL, H.B., GUPTA, A.K., BHATNAGAR A.K., Trans IChemE, **85 (B5)**, 2007, p. 458
5. RICHARDSON, Y., BLIN, J., VOLLE, G., MOTUZAS, J., JULBE A., Applied Catalysis A: General, **382**, 2010, p. 220
6. ZANZI, R., Pyrolysis of Biomass, Dissertation, Royal Institute of Technology, Stockholm, 2001
7. GONZALEZ, J.F., ENCINAR, J.M., CANITO, J.L., SABIO, E., CHACON, M., J. Anal. Appl. Pyrol., **67**, 2003, p. 165
8. XIU, S., LI, Z., LI, B., YI, W., BAI, X., Fuel, **85**, 2006, p. 664
9. ACIKGOZ, C., ONAY, O., KOCKAR, O.M., J. Anal. Appl. Pyrolysis, **71**, 2004, p. 417
10. ÇAGLAR, A., DEMIRBAS, A., Energ. Convers. Manage., **43**, 2002, p. 109
11. ÇAGLAR A., DEMIRBAS, A., Energ. Convers. Manage., **43**, 2002, p. 489
12. DAMARTZIS, T., IOANNIDIS, G., ZABANIOTOU, A., Chem. Eng. J., **136**, 2008, p. 320
13. DEMIRBAŞ, A., Energ. Convers. Manage., **43**, 2002, p. 897
14. DEMIRBAŞ, A., Energ. Convers. Manage., **43**, 2002, p. 1801
15. DEMIRBAŞ, A., J. Anal. Appl. Pyrolysis, **76**, 2006, p. 285
16. DI BLASI, C., SIGNORELLI, G., DI RUSSO, C., REA, G., Ind. Eng. Chem. Res., **38**, 1999, p. 2216
17. ZABANIOTOU, A., IOANNIDOU, O., Fuel, **87**, 2008, p. 834
18. YU, F., RUAN, R., STEELE, P., Trans. ASABE, **51**, 2008, p. 1023
19. DOBRE, T., PÂRVULESCU, O.C., IAVORSCHI, G., STOICA, A., STROESCU, M., International Journal of Chemical Reactor Engineering, **8**, 2010, p. 1968
20. DOBRE, T., PÂRVULESCU, O.C., CEATRĂ, L., STROESCU, M., IAVORSCHI, G., 2010, 6th European Meeting on Chemical Industry and Environment (EMChIE), Mechelen, Belgium, Conference Proceedings, **1**, p. 605
21. BRADBURY, A.G.W., SAKAI, Y., SHAFIZADEH, F., J. Appl. Polym. Sci., **23**, 1979, p. 3271
22. KOUFOPANOS, C.A., PAPAYANNAKOS, N., MASCHIO, G., LUCCHESI, A., Can. J. Chem. Eng., 69, 1991, p. 907
23. HASELI, Y., VAN OIJEN, J.A., DE GOEY, L.P.H., J. Anal. Appl. Pyrolysis, **90**, 2011, p. 140
24. PIDDUBNIAK, O., LEDAKOWICZ, S., NOWICKI, L., International Journal of Heat and Mass Transfer, **54**, 2011, p. 338
25. SIMMONS, G. M., GENTRY, M., J Anal. Appl. Pyrolysis, **10**, 1986, p. 117
26. PÂRVULESCU, O.C., DOBRE, T., CEATRĂ, L., IAVORSCHI, G., MIREA, R., Rev. Chim. (Bucharest), **62** , no. 1, 2010, p. 89
27. ABOULKAS, A., EL HARFI, K., EL BOUADILI, A., NADIFIYINE, M., BENCHANAA, M., MOKHLISSE, A., Fuel Process. Technol., **90**, 2009, p. 722
28. GUINESI, L.S., ROZ, A.L., CORRADINI, E., MATTOSO, L.H.C., TEIXEIRA, E.M., CURVELO, A.A.S., Thermochim. Acta, **447**, 2006, p. 190
29. HU, S., JESS, A., XU, M., Fuel, **86**, 2007, p. 2778
30. IOANNIDOU, O., ZABANIOTOU, A., Renew. Sustain. Energ. Rev., **11**, 2007, p. 1966
31. SUAREZ-GARCIA, F., MARTINEZ-ALONSO, A., TASCON, J. M. D., J. Anal. Appl. Pyrol., **62**, 2002, p. 93

Manuscript received: 8.09.2011